Advances in Aerospace Science and Technology, 2022, 7, 123-134
https://www.scirp.org/journal/aast
ISSN Online: 2473-6724
ISSN Print: 2473-6708

# Prediction of Aerothermal Environment and Heat Transfer for Hypersonic Vehicles with Different Aerodynamic Shapes Based on C++

**Tianqiang Huang, Guoyi He, Qi Wang**

Nanchang Hangkong University, Faculty of Flight Engineering, Nanchang, China
Email: hegy509@163.com

**How to cite this paper:** Huang, T.Q., He, G.Y. and Wang, Q. (2022) Prediction of Aerothermal Environment and Heat Transfer for Hypersonic Vehicles with Different Aerodynamic Shapes Based on C++. *Advances in Aerospace Science and Technology*, **7**, 123-134.
https://doi.org/10.4236/aast.2022.73008

**Received:** August 18, 2022
**Accepted:** September 26, 2022
**Published:** September 29, 2022



## Abstract

This research paper discusses constructing a unified framework to develop a full-rate scheme for hypersonic heating calculations. The method uses a flow tracing technique with normal phase vector adjustment in a non-structured delineated grid combined with empirical formulations for convective heat transfer standing and non-standing heat flow engineering. This is done using dev-C++ programming in the C++ language environment. Comparisons of the aerodynamic thermal environment with wind tunnel experimental data for the Space Shuttle and Apollo return capsules and standing point heat transfer measurements for the Fire II return capsule was carried out in the hypersonic Mach number range of 6 - 35 Ma. The tests were carried out on an 11th Gen Intel(R) Core(TM) i5-1135G7 processor with a valuable test time of 45 mins. The agreement is good, but due to the complexity of the space shuttle tail, the measurements are still subject to large errors compared to wind tunnel experiments. A comparison of the measured Fire-II return capsule standing-point heat values with the theory for calculating standing-point heat fluxes simulated using Fay & Riddell and wind tunnel experiments is provided to verify the validity of this procedure for hypersonic vehicle heat transfer prediction. The heat fluxes assessed using this method for different aerodynamic profiles of hypersonic vehicles agree very well with the theoretical solution.

## Keywords

Hypersonic, C++, Aerodynamic Heating, Reentry Vehicle, Aerodynamic Thermal Environment

## 1. Introduction

Surface heat flux assessment of aerodynamic surfaces is crucial for hypersonic vehicles and contributes to the design and development of high-speed vehicles [1]. To this end, accurate prediction of heat transfer rates is a significant issue for researchers and developers working within current space programmes [2]. A low computational cost convective heat transfer technique based on the optimisation of convective heat transfer coefficients has been proposed by Avallone [3] *et al.* Recent work on the numerical study of convective and hypersonic flows includes the work of Ryzhkov and Kuzenov [4]. A modified non-equilibrium model for oxygen, vital for hypersonic cruise vehicles, has recently been proposed by Kim [5] *et al.* Reactive gas-surface interactions were investigated by Yang [6] *et al.* and Bouyahiaoui [7] [8] using an open-source solver for $CO_2$ flow, which provides a good model for the Martian atmosphere. Steffen [9] performed temperature-sensitive paint (TSP) tests to obtain the convective parameter ρck for measuring various objects in hydrodynamic and aerodynamic experiments Saiprakash *et al.* discussed the effect of angle of attack and obtuseness on the heating rate distribution of an obtuse cone model at hypersonic velocities [10]. Estruch-Sample [11] [12] discussed a more detailed description of the understanding of hypersonic heat flow and the proposal of an engineering method to predict the location and magnitude of the highest heat transfer rate. In 2020, Shen [13] presented the effect of angle of attack variations on a hypersonic vehicle's incoming heat transfer and thermal protection system (TPS) under off-design conditions. Moreira numerically simulated the atmospheric re-entry vehicle SARA using the Navier-Stokes equations using the finite volume method [14]. Mohammed and Kim *et al.* used aerodynamic thermal load progenitors and considered local piston theory and the Eckert reference enthalpy temperature method to effectively predict the temperature variation of the entire mission trajectory of a hypersonic vehicle [15] [16].

Many researchers have proposed several solutions to the problem of aerodynamic heating of hypersonic vehicle surfaces. These include research work using numerical computational methods, indirect measurements of the heat flow distribution on the surface of an object using temperature-sensitive coatings, and discussions of the effects of different wind conditions on the heating rate distribution of the classical model. There has never been a systematic, efficient and low-cost solution. In this paper, a C++-based aerodynamic thermal calculation program is constructed to obtain the surface heat flow through the surface element method, radius of curvature calculation, and streamline tracking techniques for the Space Shuttle Orbiter, AS-202, and FIRE-II, respectively. The calculated results are in good agreement with the wind tunnel experimental results.

## 2. Definition of a Computational Model

In this paper, NASA's open source parametric geometric modelling software Open VSP (Open Vehicle Sketch Pad) was used for the parametric description and automatic generation of the 3D CAD models of the Apollo Command Module (AS-202 Flight Test) [17] and Space Shuttle Orbiter [18]. The open source program NETGEN [19] was used to automate the meshing of the generated CAD shapes. The meshing diagrams for the three models are shown in **Figures 1-3**.

## 3. Engineering Calculation Methods

### 3.1. Surface Element Method and Surface Pressure Calculation

The essence of the solution by the surface element method is the assumption that the aerodynamic properties of each grid are only related to the parameters of the free incoming flow and the geometrical parameters of the current grid

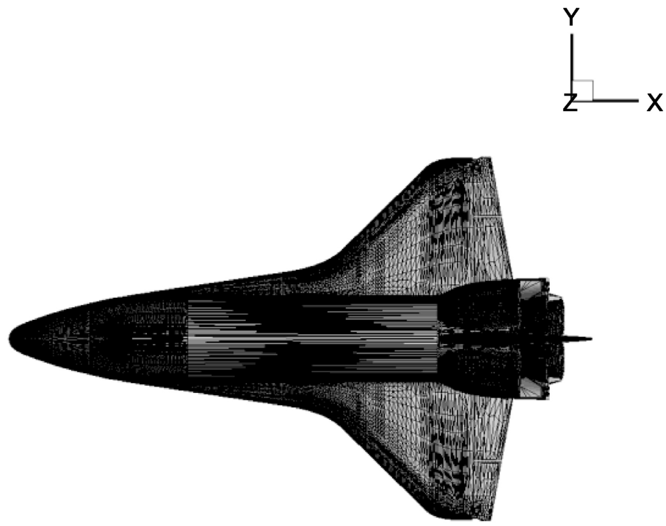


**Figure 1.** Space shuttle grid division.

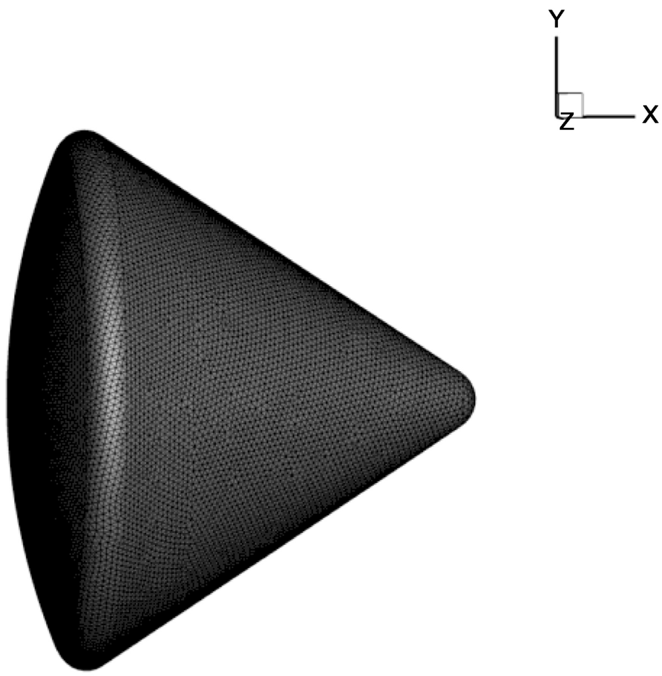


**Figure 2.** Apollo grid division.

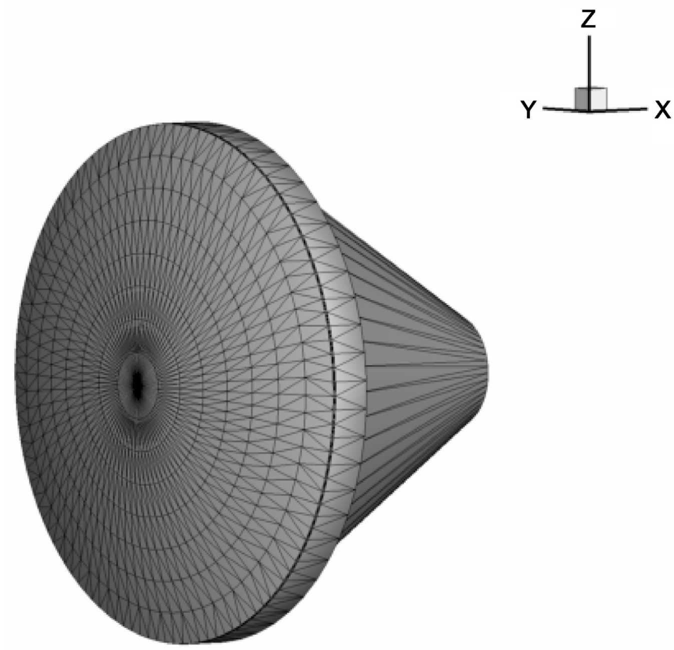


**Figure 3.** Fire-II grid division.

(area and direction of the outer normal), and that the other grids do not interfere with the existing grid. The surface pressure coefficients are calculated, and the aerodynamic coefficients are obtained by integration [20]. The entropy on each panel is equal to the post-normal surge entropy is the entropy assumption. The known pressure and entropy values in each panel fix the thermodynamic state of the boundary layer edge. A table look-up procedure for the data created using the Gordon and McBride (CEA) code in reference [21] was used to calculate the remaining thermodynamic properties, such as temperature and enthalpy.

$$C_P = \frac{2(P - P_\infty)}{\rho_\infty V_\infty^2} \tag{1}$$

$$P = \rho RT \tag{2}$$

$$h_w = c_p T \tag{3}$$

$C_p$ is the local friction coefficient and $R$ is the gas constant. According to the cold wall assumption, let the wall temperature be 300 K, can calculate the wall enthalpy $H_w$. Adiabatic wall enthalpy calculation formula is

$$H_w = r(H_0 - H_e) + H_e \tag{4}$$

$$H_0 = H_e + \frac{V_e^2}{2} \tag{5}$$

$$r = Pr^{1/2} \quad \text{(Laminar flow)} \tag{6}$$

The relevant factorless parameter is assumed to be constant, taking $Pr = 0.71$ [22].

For hypersonic Mach numbers, the inviscid solutions are based on independent panel methods such as the modified Newtonian volume, tangent cone and tangent wedge formulations. Using the Dejarnetle formula for the windward side and the Plante-Meyer expansion wave method for the leeward side. The independent panel methods provide the pressures at each surface triangle. Where $\theta$ is the angle of impact.

$$C_P = C_{p\max}\left(1 - D\cos^G\theta\right) \tag{7}$$

$$\begin{aligned} G = {} & 2.6054749 - 0.465998 M\alpha_\infty + 0.09309305 M\alpha_\infty^2 \\ & - 0.00817329 M\alpha_\infty^3 + 0.00026447 M\alpha_\infty^4 \end{aligned} \tag{8}$$

$$D = \begin{cases} 1.570367 - 0.565058 M\alpha_\infty + 0.2071167 M\alpha_\infty^2 & \\ -0.0341656 M\alpha_\infty^3 + 0.000210593 M\alpha_\infty^4 & 1.5 \le M\alpha \le 3.8 \\ 1.0081057 - 0.0132323 M\alpha_\infty + 0.00164956 M\alpha_\infty^2 & \\ -0.00006797 M\alpha_\infty^3 & 3.8 < M\alpha \le 10 \end{cases} \tag{9}$$

### 3.2. Surface Pneumatic Thermal Environment and Heat Flow Calculations

Based on a comparative study of the accuracy of different standing heat flow formulas in the relevant literature [23], the Kemp-Riddell formula was selected for this paper to calculate.

$$q_{ws} = \frac{131884.2}{\sqrt{R_N}}\left(\frac{\rho_\infty}{\rho_0}\right)^{0.5}\left(\frac{v_\infty}{v_c}\right)^{3.25}\left(1 - \frac{h_w}{h_s}\right) \tag{10}$$

where $\rho_0$ = 1.225 kg/m$^3$, $v_c$ = 7900 m/s, $R_N$ is the radius of curvature of the standing point (m); $q_{ws}$ is the standing point heat flow density, and $h_s$ is the standing point hysteresis enthalpy.

In this paper, the Voronoi method of Meyer [24] is chosen to calculate the best-fitting surface using sufficient adjacent triangles in the least squares sense. The principal curvature is then calculated directly from this cubic surface. The average value of the principal curvature is used to determine the local radius. The curvature and radius of curvature are calculated as

$$k_H\left(V_i\right) = \frac{1}{4A_{mixed}} \sum_{V_j \in neighbor(V_i)} \left(\cot\alpha_{ij} + \cot\beta_{ij}\right)\left(\left(V_i - V_j\right) \times \vec{n}\right) \tag{11}$$

$$R_N = \frac{1}{k_H} \tag{12}$$

where the mixing area is the area of the red area in **Figure 4**.

## 4. Results and Analysis of Program Calculations

The next set of results is for the Space Shuttle Orbiter module. The re-entry conditions are listed in **Table 1**. The first set of results is for a Mach number of 6.02 for the Shuttle orbiter, a free-stream density of 4.1763e−03 kg/m$^3$, and a free-stream temperature of 254.26 K and an angle of attack of 29.18˚. Again the results of this paper's method were compared with the predictions of CBAERO

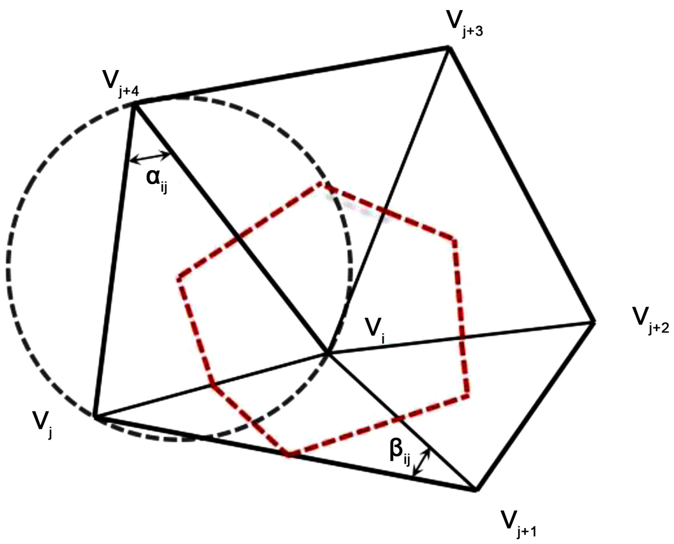


Figure 4. Schematic diagram of the Voronoi method for finding the curvature of a surface element.

Table 1. Three types of program verification in this article.

| Name | Simulation of conditions | | | | |
|---|---|---|---|---|---|
| | Mesh | Ma | Ma A0A | T | ρ |
| Space Shuttle Orbiter | 114,960 | 6.02 | 29.18 | 254.2 | 4.18e−3 |
| AS-202 | 33,438 | 10 | 18.2 | 274 | 1.16e−3 |
| Fire-II | 24,467 | 25.6 | 0 | 253 | 6.05e−3 |

and the high-fidelity CFD code DPLR of NASA Ames. The unstructured surface mesh of the space shuttle model contains 114,960 triangles. It took approximately 45 minutes to run a solution on a 2.6 GHz Dell laptop.

Figure 5 shows the surface temperatures predicted using the methods in this paper. Details of the centreline pressure and temperature distributions are shown in Figure 6 and Figure 7. This paper does a good job of predicting centreline pressure and it also does a good job of predicting windward centreline temperature. On the leeward side of the vehicle, a trend towards increased heating on the vertical tail is captured, but the change in temperature and magnitude is not accurately predicted.

Figures 8-12 show details of pressure and temperature along the vehicle at constant "x" slices of 8 m and 28 m. Along the x = 8 m cut, the paper's method is slightly better at predicting peak pressures but does a reasonable job of predicting windward and downwind temperatures. Along the x = 28 m cut, the method in this paper generally does a good job of predicting pressure and capturing peak temperatures on the windward surface, but does not capture peak heating points on the leeward surface.

The Apollo surface triangulation delineated in this paper contains 33,438

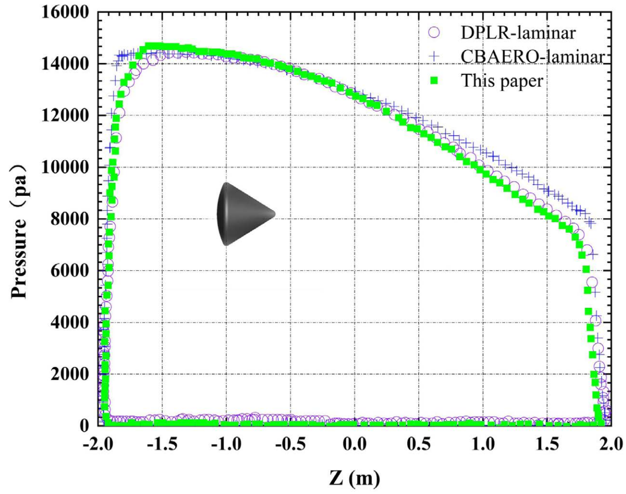


**Figure 5.** Apollo 18.6˚ centreline pressure distribution.

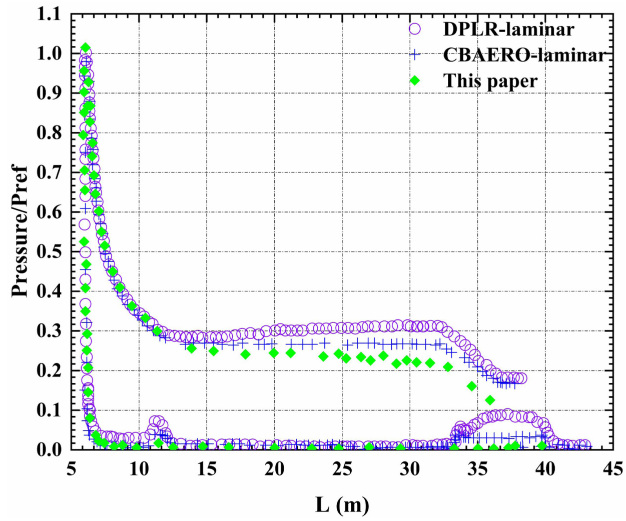


**Figure 6.** Space Shuttle 30˚ centreline pressure diagram.

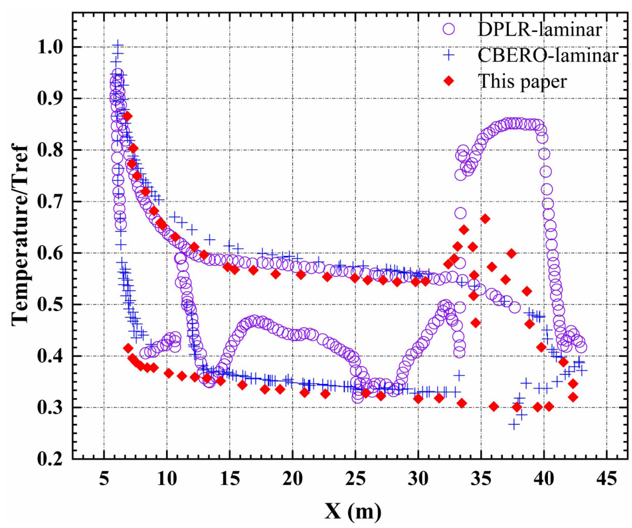


**Figure 7.** Space Shuttle 30˚ centreline temperature graph.

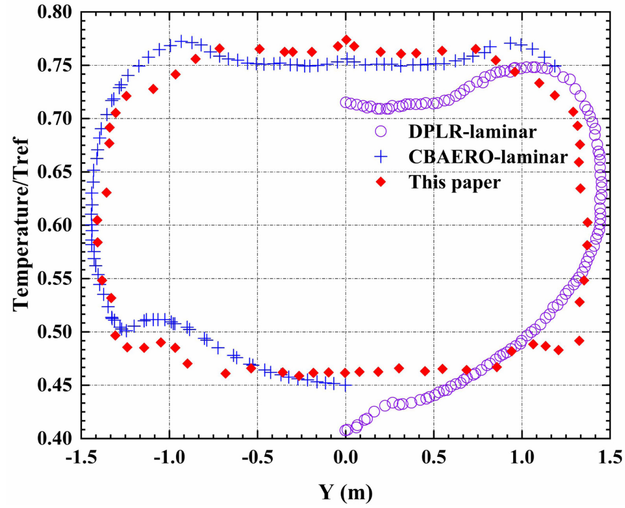


**Figure 8.** Space Shuttle 6 Ma 30˚ 8 m temperature profile.

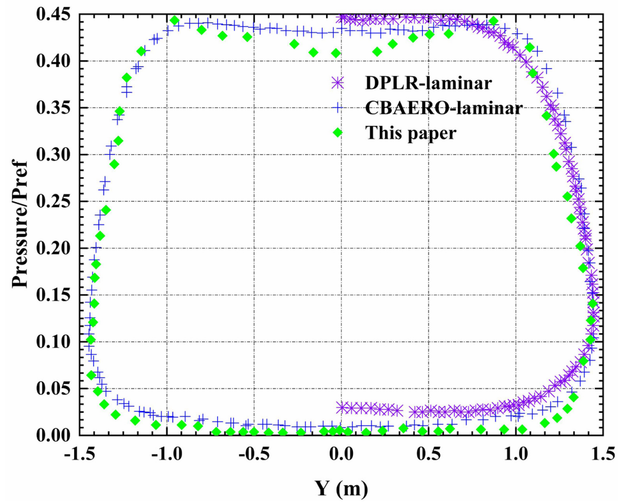


**Figure 9.** Shuttle 6 Ma 30˚ 8 m pressure distribution.

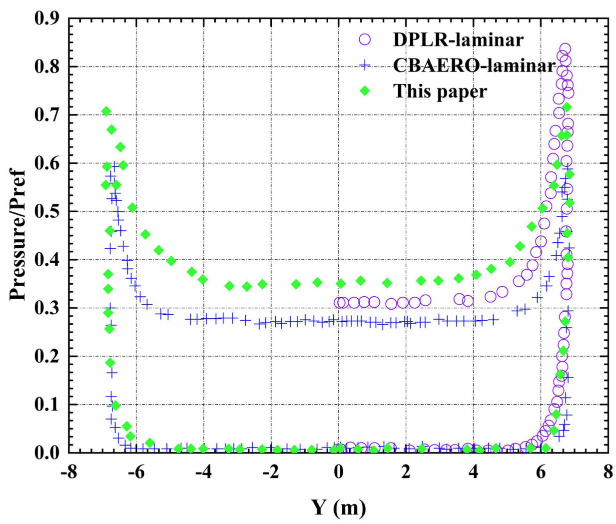


**Figure 10.** Space Shuttle 6 Ma 30˚ 28 m pressure distribution.

triangles, as shown in **Figure 2**. **Figure 12** shows the surface pressure distribution along the Apollo centreline and **Figure 5** compares the results of this paper's solution with those of CBAERO and DPLR along the vehicle centreline. In general, the pressure field is well predicted, as is the overall temperature on the heat shield. The method in this paper does capture the peak heating in the shoulder of the return capsule, but the distribution beyond the shoulder is not consistent with the DPLR results.

To validate the standing heat flow density method, this paper compares data from the FIRE-II flight experiment, shown in **Figure 13**. The FIRE-II project was a suborbital re-entry test conducted by NASA in 1965 using a scaled-down

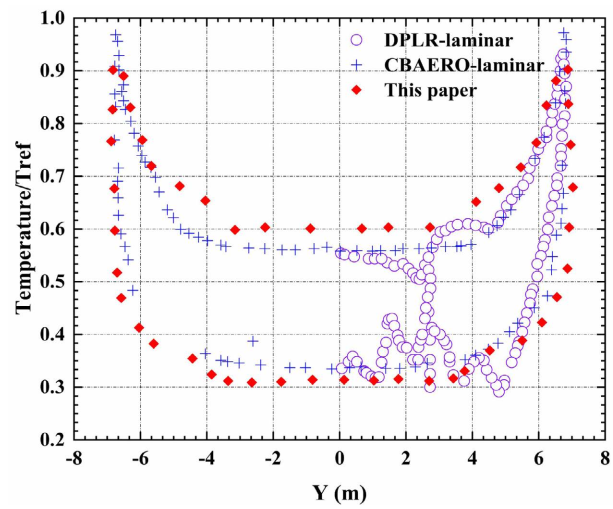


**Figure 11.** Space Shuttle 6 Ma 30˚ 28 m temperature profile.

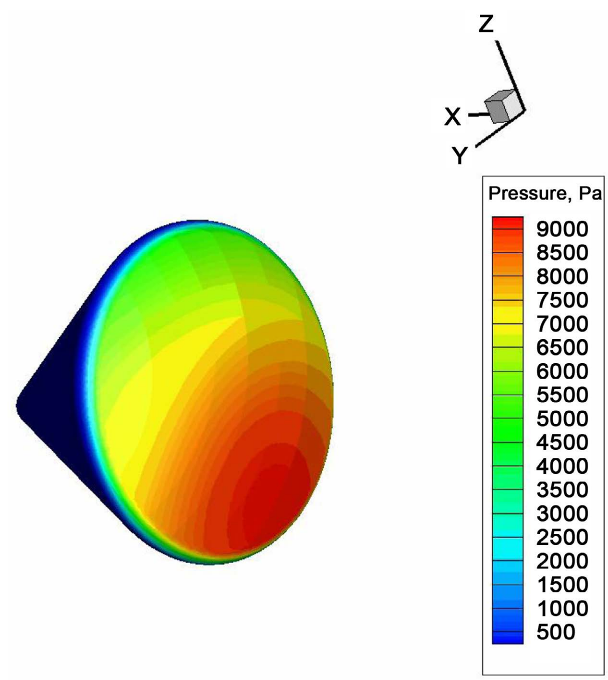


**Figure 12.** Apollo Ma = 25.6 17.8˚ surface pressure.

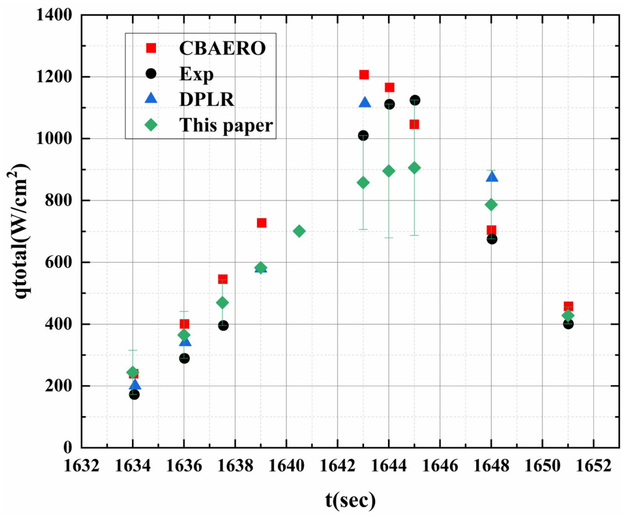


**Figure 13.** Fire-II complete standing heat flow diagram acknowledgements.

model of the Apollo command module at re-entry velocity in order to investigate the flight environment of re-entry bodies [25]. The geometrical data were obtained from M. Wright's paper and were chosen for a flight condition of 1651s with density 1 = 6.05e−3 kg/m$^3$, and incoming velocity V1 = 6.19 km/s and temperature T1 = 253 K. The flight experiment data were 405.4 w/cm$^2$, and the standing heat flow density derived from this method was 428.1 w/cm$^2$, an error of 5.60%. cm$^2$, with an error of 5.60%, meets the engineering calculation accuracy requirements.

## 5. Conclusions

This paper used a C++-based aerodynamic engineering calculation program to predict three re-entry vehicle shapes, including the return module and re-entry vehicle, flying at speeds from Mach 6 to Mach 35. In the Fire-II flight state of 1639s-1643s, the air is subjected to pyrolysis and chemical reactions that affect the prediction of heat flow at the stationary point, which the authors will consider in their subsequent work.

The ability of the method to predict the convective heating, and thermodynamic environment of the vehicle, based on the vehicle shape, and flight speed, is compared with high fidelity CFD and flight test data. As a tool for rapid engineering methods, comparison with flight test data was found to be "reasonable" for predicting complex flow fields for various re-entry vehicles. The short time required to predict a complete set of flight data using this method is an effective tool for predicting the complete aerothermodynamic environment early in the conceptual and preliminary design phase of a hypersonic vehicle.

## Conflicts of Interest

The authors declare no conflicts of interest regarding the publication of this paper.

## References


[1] Kumar, R. (2022) Assessments of Surface Heat Flux from Rapid Temperature Sensors at Various Angles of Attack over a Plate. *Journal of Thermal Analysis and Calorimetry*, **147**, 11493-11506.

[2] Wang, Q., *et al.* (2016) Comparative Study on Aerodynamic Heating under Perfect and Nonequilibrium Hypersonic Flows. *Science China Physics, Mechanics & Astronomy*, **59**, Article ID: 624701. https://doi.org/10.1007/s11433-015-5708-1

[3] Avallone, F., *et al.* (2015) A Low-Computational-Cost Inverse Heat Transfer Technique for Convective Heat Transfer Measurements in Hypersonic Flows. *Experiments in Fluids*, **56**, Article No. 86. https://doi.org/10.1007/s00348-015-1951-5

[4] Ryzhkov, S.V. and Kuzenov, V.V. (2019) New Realization Method for Calculating Convective Heat Transfer near the Hypersonic Aircraft Surface. *Zeitschrift für angewandte Mathematik und Physik*, **70**, Article No. 46. https://doi.org/10.1007/s00033-019-1095-1

[5] Kim, J.G., Kang, S.H. and Park. S.H. (2020) Thermochemical Nonequilibrium Modeling of Oxygen in Hypersonic Air Flows. *International Journal of Heat and Mass Transfer*, **148**, Article ID: 119059. https://doi.org/10.1016/j.ijheatmasstransfer.2019.119059

[6] Yang, X.F., *et al.* (2020) Reacting Gas-Surface Interaction and Heat Transfer Characteristics for High-Enthalpy and Hypersonic Dissociated Carbon Dioxide Flow. *International Journal of Heat and Mass Transfer*, **146**, Article ID: 118869. https://doi.org/10.1016/j.ijheatmasstransfer.2019.118869

[7] Bouyahiaoui, Z., *et al.* (2020) Prediction of the Flow Field and Convective Heating during Space Capsule Reentry Using an Open Source Solver. *International Journal of Heat and MassTransfer*, **148**, Article ID: 119045. https://doi.org/10.1016/j.ijheatmasstransfer.2019.119045

[8] Bouyahiaoui, Z., Haoui, R. and Zidane. A. (2020) Numerical Investigation of a Hypersonic Flow around a Capsule in $CO_2$-$N_2$ Environment. *European Journal of Mechanics-B/Fluids*, **80**, 146-156. https://doi.org/10.1016/j.euromechflu.2019.12.009

[9] Risius, S., *et al.* (2017) Determination of Heat Transfer into a Wedge Model in a Hypersonic Flow Using Temperature-Sensitive Paint. *Experiments in Fluids*, **58**, Article No. 117. https://doi.org/10.1007/s00348-017-2393-z

[10] Saiprakash, M., *et al.* (2019) Effects of Angle of Attack and Bluntness on Heating Rate Distribution of Blunt Models at Hypersonic Speeds. *Fluid Dynamics*, **54**, 850-862. https://doi.org/10.1134/S0015462819060090

[11] Estruch, D., *et al.* (2010) Hypersonic Interference Heating in the Vicinity of Surface Protuberances. *Experiments in Fluids*, **49**, 683-699. https://doi.org/10.1007/s00348-010-0844-x

[12] Estruch, D. (2009) Hypersonic Interference Aerothermodynamics. Diss. PhD Thesis, Department of Aerospace Sciences, Cranfield University, Bedford.

[13] Shen, B.-X., Liu, H.-P. and Liu, W.-Q. (2020) Influence of Angle of Attack on a Combined Opposing Jet and Platelet Transpiration Cooling Blunt Nose in Hypersonic Vehicle. *Journal of Zhejiang University—Science A*, **21**, 761-769. https://doi.org/10.1631/jzus.A1900514

[14] Moreira, F.C., Wolf, W.R. and Azevedo, J.L.F. (2022) Thermal Analysis of Hypersonic Reactive Flows on the SARA Brazilian Satellite Reentry Trajectory. *Journal of the Brazilian Society of Mechanical Sciences and Engineering*, **44**, Article No. 36. https://doi.org/10.1007/s40430-021-03336-3

[15] Mohammed, H.A., Salleh, H. and Yusoff, M.Z. (2010) Fast Response Surface Temperature Sensor for Hypersonic Vehicles1. *Instruments and Experimental Techniques*, **53**, 153-159. https://doi.org/10.1134/S0020441210010288

[16] Kim, G., *et al.* (2020) Efficient Prediction of the Temperature History of a Hypersonic Vehicle throughout the Mission Trajectory with an Aerodynamic Thermal Load Element. *International Journal of Aeronautical and Space Sciences*, **21**, 363-379. https://doi.org/10.1007/s42405-019-00225-x

[17] Wright, M., Prabhu, D. and Martinez, E. (2004) Analysis of Afterbody Heating Rates on the Apollo Command Modulels, Part I: AS-202. 37*th AIAA Thermophysics Conference*, Portland, 28 June 2004-1 July 2004, 16. https://doi.org/10.2514/6.2004-2456

[18] De Venzia, J., Wang, J.M. and Caram, J.M. (1995) Space Shuttle Orbiter Wing Leading Edge Heating Predictions and Measurements. NASA CP 3248, 741-809.

[19] Yilmaz, Y. and Ozturan, C. (2015) Using Sequential NETGEN as a Component for a Parallel Mesh Generator. *Advances in Engineering Software*, **84**, 3-12. https://doi.org/10.1016/j.advengsoft.2014.12.013

[20] Huang, T.Q., He, G.Y. and Wang, Q. (2022) Calculation of Aerodynamic Characteristics of Hypersonic Vehicles Based on the Surface Element Method. *Advances in Aerospace Science and Technology*, **7**, 112-122. https://doi.org/10.4236/aast.2022.72007

[21] Gordon, S. and McBride, B.J. (1994) Computer Program for Calculation of Complex Chemical Equilibrium Compositions and Applications. Part 1: Analysis. No. NAS 1.61, 1311.

[22] Li, J.L., *et al.* (2012) Fast Engineering Estimation of Aerodynamics and Heat for Hypersonic Vehicles with Complex Shapes. *Journal of National University of Defense Technology*, **34**, 5.

[23] Huo, L. (2012) Aero-Thermal Fast Engineering Estimation and Thermal Response Analysis of Complex Shape Hypersonic Vehicle. University of National Defense Science and Technology, Beijing.

[24] Meyer, M., *et al.* (2003) Discrete Differential-Geometry Operators for Triangulated 2-Manifolds. In: Hege, H.-C. and Polthier, K., Eds., *Visualization and Mathematics III*, Springer, Berlin, 35-57. https://doi.org/10.1007/978-3-662-05105-4_2

[25] Wright, M., Loomis, M. and Papadopoulos, P. (2003) Aerothermal Analysis of the Project Fire II Afterbody Flow. *Journal of Thermophysics and Heat Transfer*, **17**, 240-249. https://doi.org/10.2514/2.6757